https://ntrs.nasa.gov/search.jsp?R=19840019213 2020-03-22T09:23:53+00:00Z

N84 27281

# AN IMPROVED DUAL-FREQUENCY TECHNIQUE FOR THE REMOTE SENSING OF OCEAN CURRENTS AND WAVE SPECTRA

Dale L. Schuler
Wah P. Eng

U. S. Naval Research Laboratory
Washington, D. C. 20375, USA

## ABSTRACT

Investigators in several countries have been studying a two-frequency microwave radar technique for the remote-sensing of directional ocean wave spectra and surface currents. This technique is conceptually attractive because its operational physical principle involves a spacial electromagnetic scattering resonance with a single, but selectable, long gravity wave. Multiplexing of signals having different spacing of the two transmitted frequencies allows measurements of the entire long wave ocean spectrum to be carried out. The two-frequency scatterometer signal/background ratio is, using conventional processing, only adequate for measurements made at or relatively near the dominant wave wavenumber when sufficient temporal averaging of spectra is employed.

A new scatterometer has been developed and experimentally tested which is capable of making measurements having much larger signal/background values than were previously possible. This new instrument couples in a hybrid fashion the resonance technique with coherent, frequency-agility radar capabilities. This scatterometer is presently configured for supporting a program of surface-current measurements. Straightforward system modifications will allow directional measurements of ocean wave slope spectra to be carried out as well as current measurements.

## 1. INTRODUCTION

The operation of dual-frequency scatterometers in detecting microwave backscatter from the ocean surface is now well understood. Such scatterometers transmit two microwave signals separated in frequency by some $\Delta f$ which is in the Megahertz range. Return signals due to each of the transmitted signals are separately received and then multiplied together. The power spectrum of the resultant output appears as shown schematically in Fig. 1. It consists of the sum of a broad background spectrum and a sharp "$\Delta k$-line". The background spectrum is the result of a convolution of the Doppler spectra of the two received microwave signals and consequently has a width of a few tens to a few hundred Hertz. The $\Delta k$-line, on the other hand, is the result of a resonance between the beat pattern of the two electromagnetic signals and the modulation pattern of the short ocean surface waves (centimetric "Bragg waves") responsible

for the backscatter. It has a width of a few tenths to a few Hertz depending on the relative speed of the microwave antenna and the ocean surface. (Plant, 1977; Alpers and Hasselman, 1978; Jackson, 1981).

The frequency of the center of the $\Delta k$-line is exactly equal to the frequency of the ocean surface wave which travels along the horizontal radar look direction and whose wavenumber, $K_w$, is $2\Delta k \cos\theta$ where $\Delta k$ is the wavenumber separation of the transmitted microwave signals and $\theta$ is the grazing angle (Plant, 1977). If a current exists on the surface, the wave of wavenumber $K_w$ will be advected by the current and its frequency in the antenna's frame of reference will change. By this means surface currents along the horizontal radar look direction can be measured using dual-frequency scatterometers (Schuler, 1978; Alpers et. al., 1980). By varying $\Delta k$, vertical profiles of horizontal currents along the radar look direction can also be determined (Schuler, et. al., 1981). One requirement for such measurements is, of course, that the $\Delta k$-line can be easily distinguished from random variance in the background level. This requirement is frequently not well satisfied and therefore severely limits applicability as well as the accuracy of the technique (Schuler, 1978).

The ratio of intensities of $\Delta k$-line and background spectrum, $\chi$, has been shown to be related to the surface wave slope spectral density $S(\vec{K}_w)$ by the equation

$$\chi = \frac{2\pi^2 |m|^2 S(\vec{K}_w) \coth^2(K_w d)}{A} \qquad (1)$$

where d is water depth, A is illuminated area, and m is the modulation transfer function relating Bragg wave modulation to the slope of the long surface wave. (Alpers and Hasselmann, 1978; Plant and Schuler, 1980). The inverse dependence of $\chi$ on A has been observed experimentally (Plant and Schuler, 1980; Johnson et al., 1982) and the equation has been shown to account well for observed values of $\chi$ (Schuler, et al., 1982; Johnson and Weissman, 1983). Alpers and Hasselman (1978) pointed out that this signal to background ratio can be increased by low pass filtering but their best estimate of such a ratio was only 1.8 for measurements from satellite altitudes. Thus, once again, the background clutter spectrum was the predominant factor limiting system performance.

In this study we have attempted to apply frequency agility techniques to dual-frequency scatterometer measurements of the ocean. In this case it is necessary to discuss two distinct types of frequency separations. In addition to the $\Delta f$ separation between transmitted pairs of signals, the carrier, or center, frequency of successive pairs of signals will be offset from one another by some $\delta f$. The sensor still remains a "dual-frequency" system in the sense that the first step in processing is to multiply returns corresponding to transmitted frequencies separated by $\Delta f$.

## 2. EXPERIMENTAL INSTRUMENTATION AND CONDITIONS

The experimental results presented in this paper were obtained at a Naval Research Laboratory field-site located on 36.6 m cliffs overlooking the Chesapeake Bay. The dual-channel, coherent radar was built at the Naval Research Laboratory and was operated at a frequency of 1.28 GHz. The basic operating parameters for this scatterometer system are given in Table 1. Both channels of the radar system are fully coherent, i.e., signal phase information is preserved. The signal coherency is retained by beating the return signal down first to IF, and then to a variable audio offset frequency (25 Hz for these experiments) which is set sufficiently high to avoid fold-over of any of the spectral components of the backscatter Doppler spectrum. This frequency-agile, dual-transmission channel radar system derives its operational flexibility from the use of an EPROM (Erasable Programmable Read-Only Memory) controlled fast-switching (20 μs/step) frequency synthesizer. The EPROM contains instructions to program the synthesizer to create a set of output carrier frequencies [$f_i$] where, i = 1, ..., $N_c$ ($1 \leq N_c \leq 98$). External counting circuits, controlled by the system PRF pulses, are used to step through the EPROM stored instructions and to continually repeat the cycle. The value of $N_c$ may be manually set to any integer value within its range. The individual output frequencies $f_i$ are held constant for 100 μs, and then are reprogrammed to a new value. A diagram showing the time dependence of transmitted frequencies corresponding to the two received channels is given in Figure 2. These diagrams resemble two "staircases" with one offset in time relative to the other by an interpulse period. Backscattered returns due to transmissions when the channel separation was $\Delta f$ were utilized in the computer processing of the data while those due to $\Delta f'$ were suppressed. A synchronization signal was derived by using digital counting circuits and a D/A converter. For the measurements reported here the difference frequency $\Delta f$ between the two L-Band channels ($f_i$, $f_i + \Delta f$) was held constant at a value of 10 MHz. This separation allowed us to resonate spatially with water waves of 15 m wavelength. This value was chosen because waves of this wavelength often are the dominant wave at the Chesapeake Bay site. The values of $f_i$ were stepped from 1.230 GHz to 1.328 GHz in 1 MHz steps. The 1 MHz spacing was selected a priori using the initial assumption (Pidgeon, 1967) that frequency changes equal to or greater than $(T)^{-1}$ (where T = the transmitted pulsewidth) would be adequate to decorrelate the backscattered returns. The work of Voles (1966) indicates that larger separations may be necessary in the presence of long waves but no experimental evidence was to substantiate that conclusion.

The processing of the fully coherent output signal $S_0(t)$ from the radar consists of three steps (1) range gating of the returns, (2) separation of the two interleaved frequency channels, and finally (3) processing of the N frequency-agile signals which occur during the transmission time of the synchronization staircase.

For the present studies, samples of the backscattered return were taken at a two-way delay of 5 μs (0.75 km) from the radar site at a grazing angle of $3^\circ$. The scattering cell dimensions were determined, at this low grazing

angle, by the pulse width (1 μs) and the azimuthal beamwidth of the antenna pattern ($6^{\circ}$ at the two-way 3 dB power point). These parameters indicate that the scattering cell was 150 m radially by 79 m azimuthally. The data reported here were taken during an eight hour period on 15 April 1982.

Wind-generated waves traveled towards shore in water which was 25 m in depth; our work indicates a dominant wavelength of 15m. The wind during the tests was from the NNE at 15-20 kts as measured by an anemometer at a height of 43 m above the sea surface. The antennas were pointed into the dominant wave direction which was observed to be from the NE. Scattered whitecaps were present. The outputs of the two radar channels as well as the synchronization signal were recorded on an analog, four-channel tape recorder operating at 30 ips. Subsequent experiments (November, 1983) conducted from the CERC Pier Duck, NC have yielded results in agreement with the measurements reported on in this paper.

## 3. DUAL FREQUENCY DOPPLER SPECTRA USING FREQUENCY-AGILE SIGNALS

The output data that were recorded consisted of a burst of up to forty-nine multiplexed, frequency-agile samples of coherent sea backscatter for both radar channels, and a synchronization signal. Our initial processing of this multiplexed time signal was both direct and simple. The output data from the two different frequency channels were passed through a laboratory multiplier and then through a low-pass filter. The time-constant of the filter was set so as to sum the N sequential frequency-agile samples together coherently. This smoothed signal was then Fourier transformed by a laboratory analyzer (Nicolet Model 444) and a power spectrum was formed. A number, generally 32, of these power spectra were then averaged together. This mode of processing is fast and effective (i.e., Δk-line detectability is greatly improved). Figure 3 illustrates the improvements in the ratio of Δk-line to background spectral intensity that can be obtained with twenty minutes of sequentially recorded data which had N = 1, 24 and 49 frequency-agile transmitted signals. It is apparent that the Δk-line processed in the conventional way (i.e., with N = 1) is almost unusably weak, whereas, the one obtained with N = 49 has been improved by almost 6.5 dB above the background intensity level. This laboratory or "immediate" mode of processing, therefore, produces a significant improvement in signal detectability.

A study was conducted to determine if the dual-frequency resonance line detectability improvements derived from the use of frequency-agility would be sufficient to obviate the need for additional temporal averaging of spectra. If such averaging could be eliminated, then a real-time sensor could be developed which would monitor Δk-line strength and line position in real-time. Real-time processing would allow ocean surface currents to be monitored continuously. The frequency-agile (N = 49) data were played through the Nicolet 444 analyzer. This analyzer has the capability of allowing selection of any of its 400 frequency bins (via placement of a cursor) for study. The output of the selected bin was available at an output port of the analyzer and was recorded on an y-t recorder. Arbitrarily selecting a detection threshold of 6 dB (line strength above the

adjacent background) the data tapes were examined to determine what fraction of the time this threshold was exceeded. The time histories of the magnitude of the peak and the background are shown in Figures 4(a) and (b).

The resonance peak exceeded this threshold 16.5% of the time when the signal was not frequency-agile (N = 1) and the signal variance was approximately equal to the mean. When the "immediate" laboratory processing was applied to the same data using N = 49 frequency-agile carrier frequencies, the short-term (<10 sec) signal variance was reduced significantly and the detection criterion was exceeded during 95% of the length of the time record.

It is useful to represent this laboratory processing mode mathematically so that it can be compared later with the processing algorithm used on the computer. The signals coming from the two system output channels (which are proportional to the coherently detected backscattered fields) may be represented as $E(t, f_n)$ and $E(t, f_n + \Delta f)$ where $f_n$ is the $n^{th}$ transmitted carrier frequency of the frequency-agile signal set. The low-frequency output of the laboratory multiplier may then be represented as

$$P_n(t) = E(t, f_n) \cdot E^*(t, f_n + \Delta f) \tag{2}$$

where, $f_n = f_o + \delta f$, $f_o = 1.23$ GHz, and $\delta f$ is stepped from 0 to N MHz in 1 MHz steps, $\Delta f = 10$ MHz.

The effect of the low-pass filter which follows the multiplier is to convolve $P_n(t)$ with a filter weighting function $W(t)$, which is the Fourier-transform of the pass-band characteristic of the filter, to form a signal $V(t)$ given by

$$V(t) = \int_{-\infty}^{\infty} P_n(\tau)\, W(t - \tau)\, d\tau$$

or, approximately

$$V(t) = \int_{T/2}^{T/2} P_n(\tau)\, W(t - \tau)\, d\tau \triangleq \sum_{n=o}^{N} P_n(t) \tag{3}$$

where,

$T = [2\Delta F_f]^{-1}$, $\Delta F_f$ = the filter 10dB cut-off width.

The signal V(t) is then processed in a laboratory Fourier analyzer (Nicolet Model 444). The output of this analyzer is a result of Fourier-transforming the input signal V(t), squaring it, and ensemble averaging over a number of data records to form

$$\overline{\left|\tilde{V}(\omega)\right|^2} = \overline{\left|\sum_{n=0}^{N} \tilde{P}_n(\omega)\right|^2}$$

$$= \overline{\sum_{n=0}^{N}\left|\tilde{P}_n(\omega)\right|^2}$$

$$+ \sum_{n=0}^{N} \sum_{\substack{\ell=0 \\ \ell \neq n}}^{N} \overline{\tilde{P}_n(\omega)\,\tilde{P}_\ell(\omega)} \qquad (4)$$

where, ~ represents a Fourier transformed quantity and $\omega$ is radian frequency. The notations $P_n(\omega)$ means the Fourier transform of the return signal pair whose carrier frequency was N MHz above a base frequency of 1230 MHz.

It should be noted that the smoothing time T of the filter need not be exactly equal to the repetition period $T_R$ of the frequency-agile signal set. If it is made longer then $T_R$ no new terms appear in Eq. (4) until the extension exceeds the temporal decorrelation time (at 1.23 GHz) of the sea itself.

Eq. (4) shows that the simple processing scheme results in an average spectrum which may be represented as a sum of auto- and cross-spectra between dual-frequency pairs having carrier frequency offsets $\delta f$ ranging from 0 to N MHz. We expect that returns due to transmitted frequencies separated by more than an inverse pulse width (in this case by more than 1 MHz) will be highly decorrelated. Thus we would expect lower background signals for cross- than auto-spectra in our sum. Since conventional processing consists of summing only auto-spectra, a net background reduction is to be expected for $\overline{|V(\omega)|^2}$.

## 5. PROPERTIES OF CROSS SPECTRA OF FREQUENCY-AGILE RETURNS

In order to investigate the validity of the results of the previous section in detail, we computed cross-spectra of $P_n$ and $P_\ell$ and compared them with the power spectrum of $P_n$ itself. To accomplish this, the data described earlier were processed using a MINC/LSI-11 computer. The procedure consisted of (1) multiplying the multiplexed signals together and, (2) demultiplexing the N product signals (Figure 5). The result of this operation was a set of individual time-series of samples of the multiplied fields $P_n(t)$ for all possible values of carrier frequency offset over the range $0 \leq n \leq N$. These time-series were then (redundantly) re-sampled and stored as disc files by the computer. It should be emphasized that these files contained return signals $P_n(t)$ which were due to transmissions whose frequency separation was constant (10 MHz) but whose carrier frequency offsets varied in 1 MHz steps. Mean square

voltage levels of these digitized signals were constant to within 10% up to 35 MHz separation. Cross- and auto-spectra were then computed using the digitized data.

In most cases, twenty-five seconds of each of two records corresponding to different carrier frequencies were transformed using a uniform time window. The product of the two transforms was computed and stored. A total of N time records were stored on disc, where N = 24 for the first data set and N=36 for the second. Therefore the number of cross-spectra between records whose carrier frequencies were separated by $\delta f$ which could be averaged together was $N-\delta f$ if $\delta f$ is in MHz. This process was repeated four times so that the total number of cross-spectra we were able to average together was $4(N-\delta f)$. For instance, the second data set yielded 144 auto-spectra which were than averaged. In one instance, discussed below, we transformed the entire 100 second data record and summed various combinations of auto- and cross-spectra. In this single case, the second data set was augmented to yield a maximum $\delta f$ of 47.

Figure 6 gives examples of spectra computed using 25 second records. Figure 6(a) is the auto-spectrum computed for the first data set with 48 degrees of freedom. Figures 6(b) and (c) show the magnitude and phase of the cross-spectrum between digital files corresponding to $\delta f$ = 10 MHz. These were computed with 28 degrees of freedom. Apparent in this figure is the decrease in background level relative to $\Delta k$-line intensity which led to the results of Section 3 (note the scale change from (a) to (b)). The phase of the cross-spectrum is quite erratic due to low number of degrees of freedom used in the computation. Note, however, that it is near zero in the frequency range of the spectral peak where the coherence between the input signals is relatively high.

Figure 7 shows the result of simulating on the computer the frequency-agile processing technique described in Section 3. The resolution is higher in this figure than the last since the whole 100 second record was transformed. In the figure, $N_s$ represents the total number of spectra averaged. Note that twice this number is not the total degrees of freedom since many records were used redundantly. Rather the number of degrees of freedom is constant at 96. The average of auto-spectra shown in Figure 7(a) correspond to the first term on the right of Eq. (4), that is to conventional dual-frequency processing. The spectrum obtained by averaging all auto- and cross-spectra from the second data set is shown in Figure 7(b). This spectrum corresponds to the frequency-agile technique output described by Eq. (4). The improvement in signal-to-background ratio for this spectrum compared to that of Figure 7(a) is 10.2 dB. This is larger than that reported in Section 2 becomes only part of the 20 minute record used in Section 2 was used here. Finally, an additional improvement in signal-to-background ratio of 2.8 dB is obtained by summing only cross-spectra as shown in Figure 7(c) and (d). Thus this method of processing results in a total improvement over conventional processing of 13 dB, again confirming that signal detectability is better for cross-spectra than auto-spectra.

## 5. CONCLUSIONS

We have demonstrated that processing dual-frequency data in a frequency-agile mode can provide significant reduction or, in some cases,

complete removal of the clutter background limitations on dual-frequency operation. The method consists of forming standard, dual-frequency products of signal pairs but then performing the final multiplication or spectral density calculation using products formed at different carrier frequencies.

When Doppler spectra for current measurements are the desired product, we have demonstrated that a simple frequency-agile processing scheme (the "immediate" laboratory mode) can produce significant improvement in signal-to-background ratio of up to 10 dB.

## 6. REFERENCES


Alpers, W. and Hasselmann, K., 1978: The Two Frequency Microwave Technique for Measuring Ocean-Wave Spectra from an Airplane or Satellite. Boundary-Layer Met. 13, 215.

Alpers, W., Schroter, J., Schlude, F., Muller, T. H. J., and Koltermann, K. P., 1980: Ocean Surface Current Measurements by an L-Band Two-Frequency Microwave Scatterometer. Radio Sci., 16, 93.

Jackson, F. C., 1981: An Analysis of Short Pulse and Dual Frequency Radar Techniques for Measuring Ocean Wave Spectra from Satellites. Radio Sci., 16, 1385.

Johnson, J. W., Weissman, D. E., and Jones, W. L., 1982: Measurement of Ocean Gravity Wave Spectrum from an Aircraft Using the Two-Frequency Microwave Resonance Technique. Int. J. Remote Sensing, 3, 383.

Johnson, J. W., and Weissman, D. E., 1983: Validation of the Two-Frequency Microwave Resonance Technique from an Aircraft: A Quantitative Estimate of the Directional Ocean Surface Spectrum. Submitted to Radio Science.

Pidgeon, V. W., 1967: Time, Frequency, and Spatial Decorrelation of Radar Sea Return. Johns Hopkins University Applied Physics Laboratory Memo No. BPD-670-7.

Plant, W. J., 1977: Studies of Backscattered Sea Return with a CW, Dual-Frequency X-Band Radar. IEEE Trans, Antennas Propagat., AP-25, 28.

Plant, W. J. and Schuler, D. L., 1980: Remote Sensing of the Sea Surface Using One- and Two-Frequency Microwave Techniques. Radio Science, 15. 605.

Schuler, D. L., 1978: Remote Sensing of Directional Gravity Wave Spectra and Surface Currents Using a Microwave Dual-Frequency Radar. Radio Science, 13, 321.

Schuler, D. L., Plant, W. J., and Eng, W. P., 1981: Remote Sensing of the Sea Using One- and Two-Frequency Microwave Techniques. Oceanography from Space, Ed. by J. F. R. Gower, Plenum Press, New York.

Schuler, D. L., Plant, W. J., Eng, W. P., Alpers, W., and Schlude, F., 1982: Dual-Frequency Microwave Backscatter from the Ocean at Low Grazing Angles: Comparison with Theory. Int. J. Remote Sensing, 3, 363.

Voles, R., 1966: Frequency Correlation of Clutter. Proc. IEEE (Letters), 54, 81.

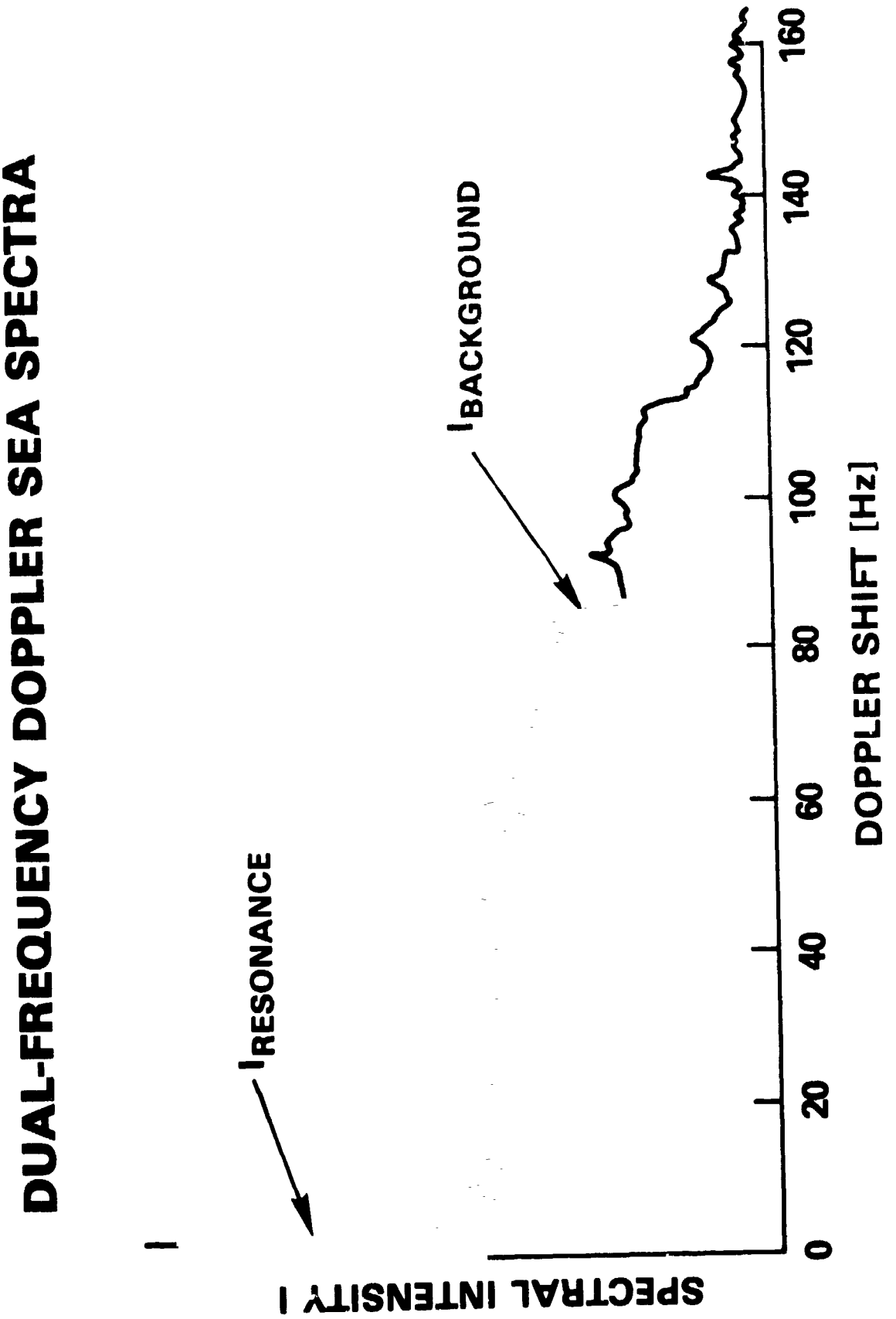


Figure 1 Power spectrum of the output of dual-frequency scatterometer.

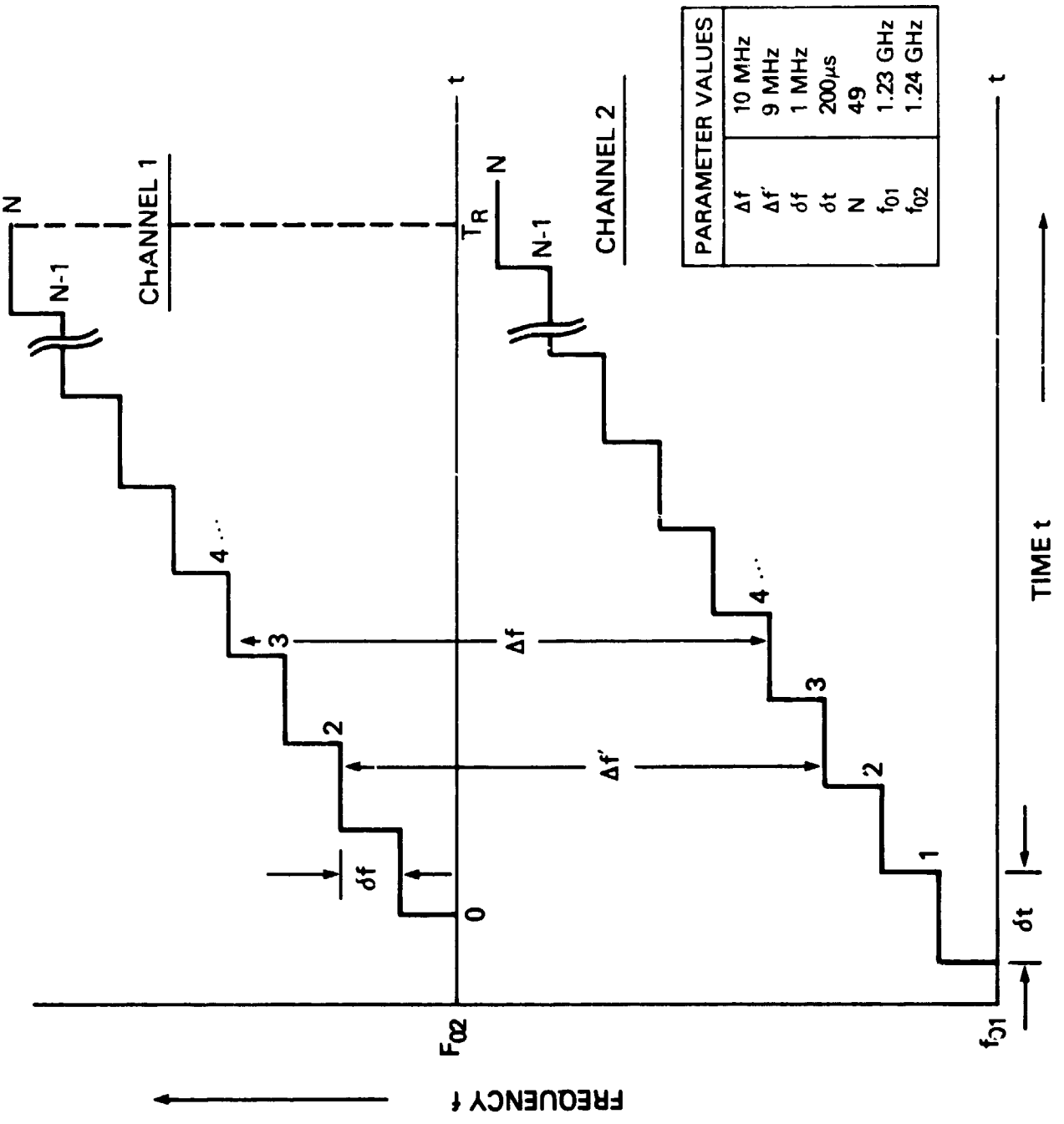


Figure 2 Received signal timing diagram for two channels of the frequency-agile, dual-frequency scatterometer used in this study.

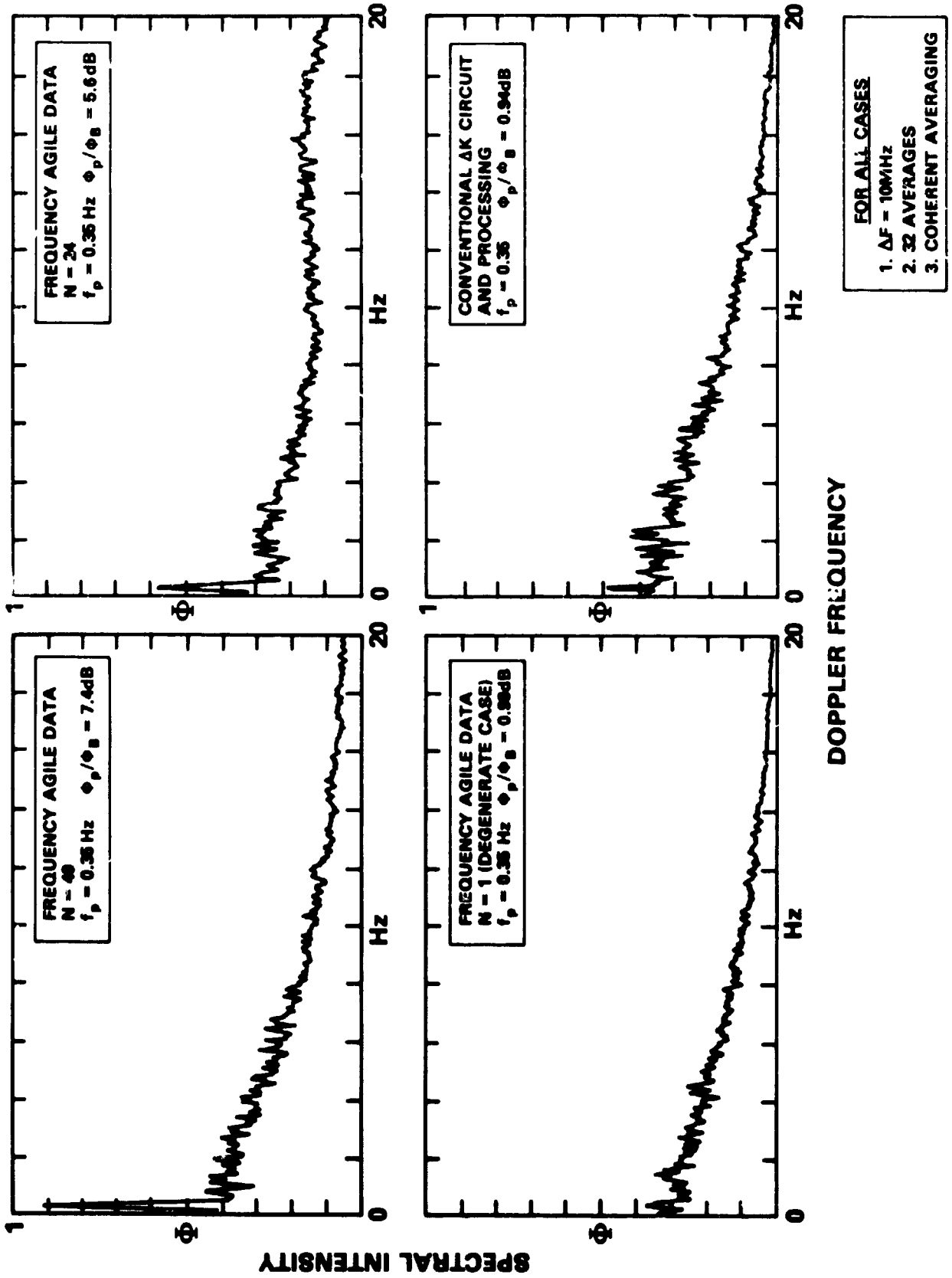


Figure 3 Output spectra of the frequency-agile, dual-frequency scatterometer using laboratory processing ("immediate" mode). (a) One carrier frequency (standard dual-frequency mode), (b) Twenty-four carrier frequencies, and (c) Forty-eight carrier frequencies.

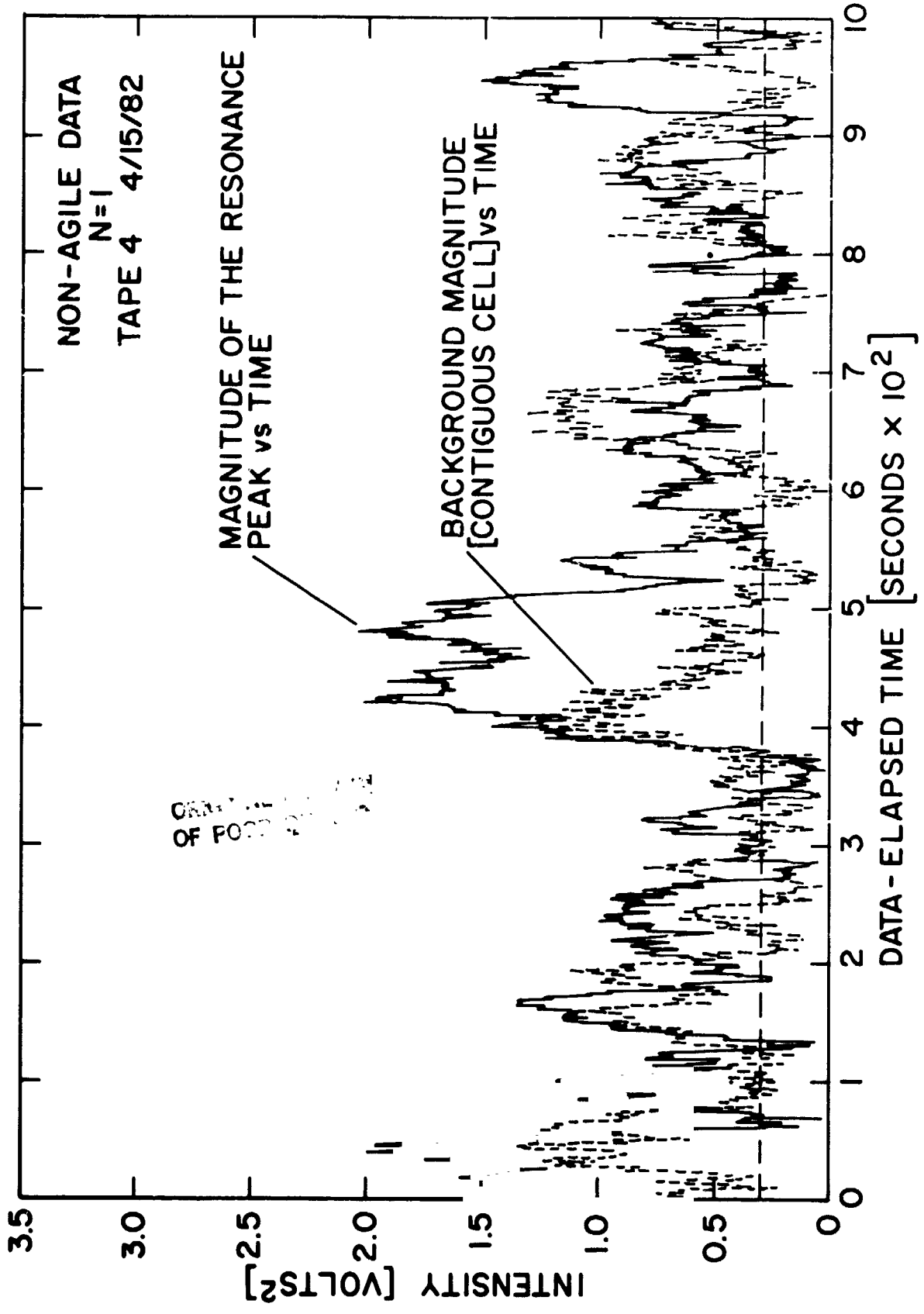


Figure 4 Time dependence of Ak-line and background spectral densities. (a) Standard dual frequency processing.

ORIGINAL PAGE IS
OF POOR QUALITY

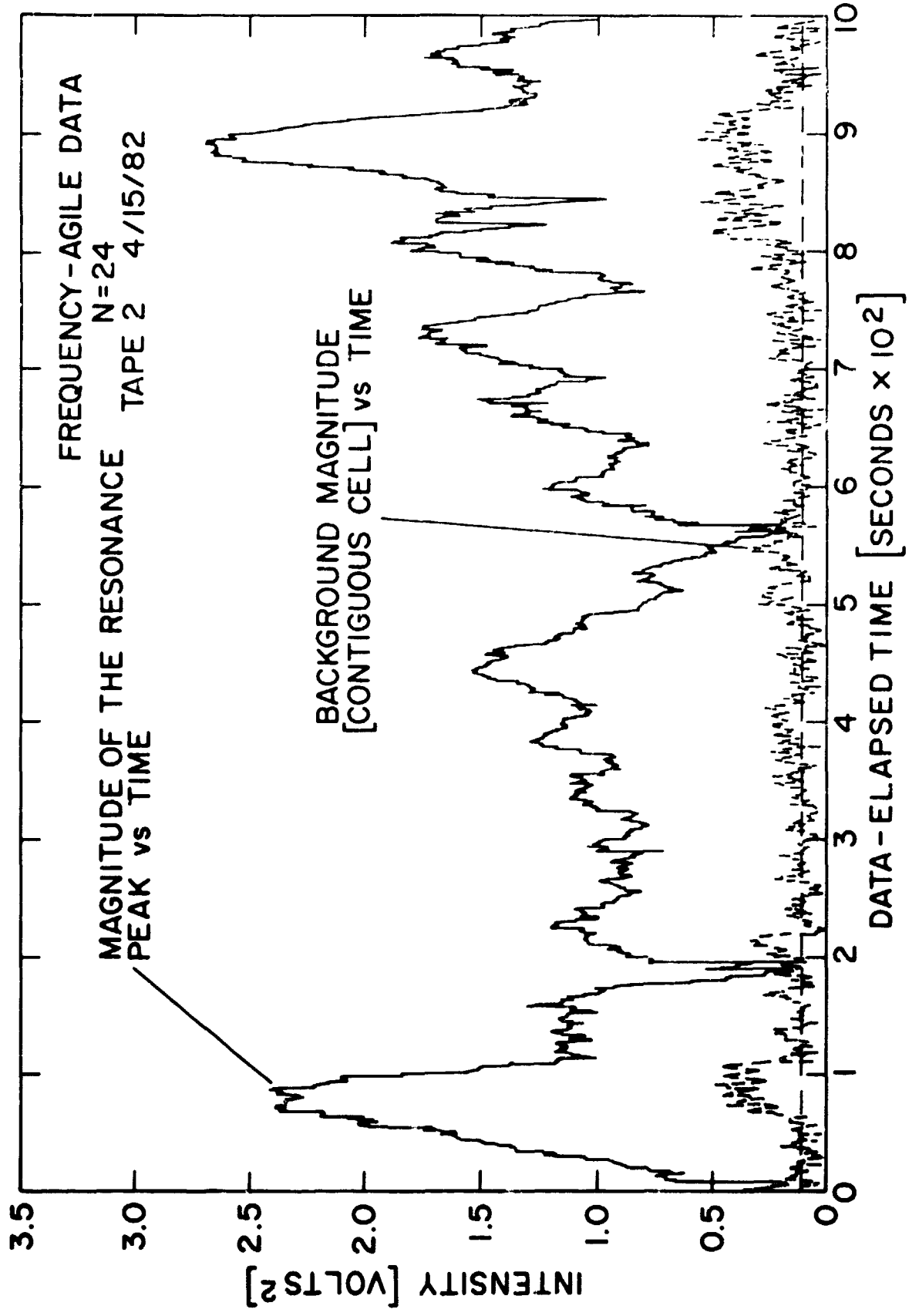


Figure 4 Time dependence of 4k-line and background spectral densities.
(b) Laboratory processing of the frequency-agile, dual-frequency scatterometer data.

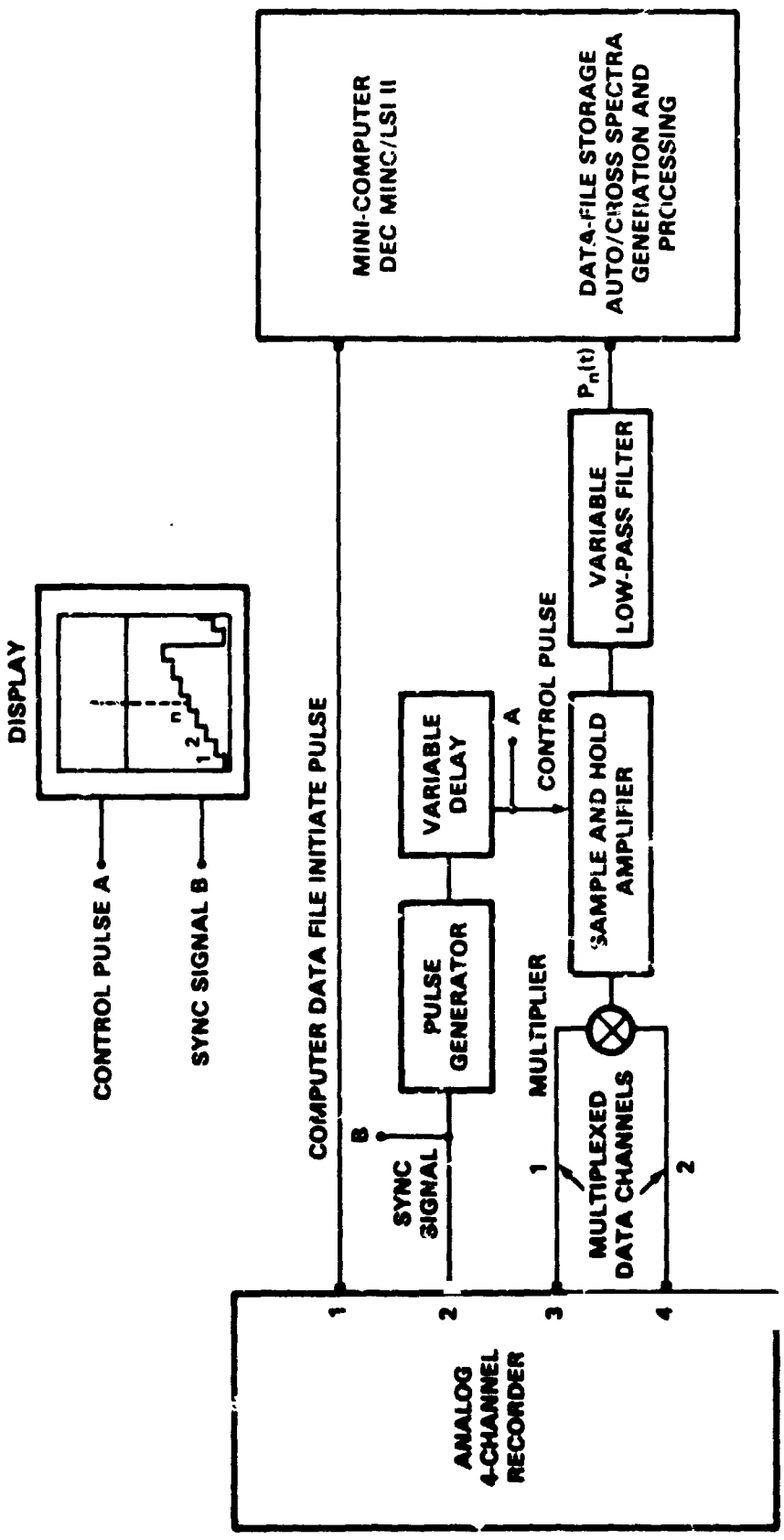


Figure 5 Schematic of signal processing for computer analysis.

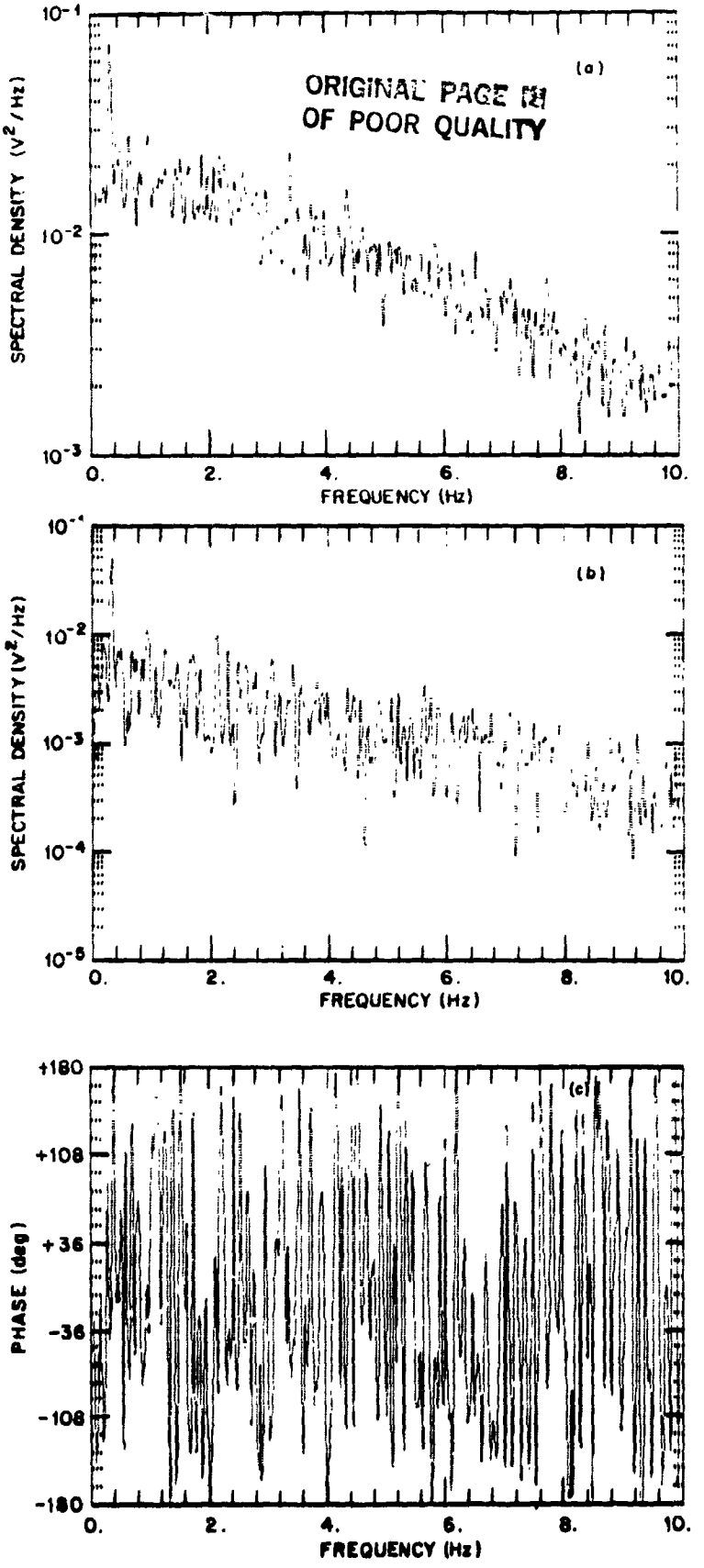


Figure 6 Auto- and cross-spectra of frequency-agile, dual-frequency scatterometer output. (a) Auto-spectrum calculated with 48 degrees of freedom. (b) Magnitude of the cross-spectrum with $\Delta f$ = 10 MHz calculated with 28 degrees of freedom. (c) Phase of the same cross-spectrum.

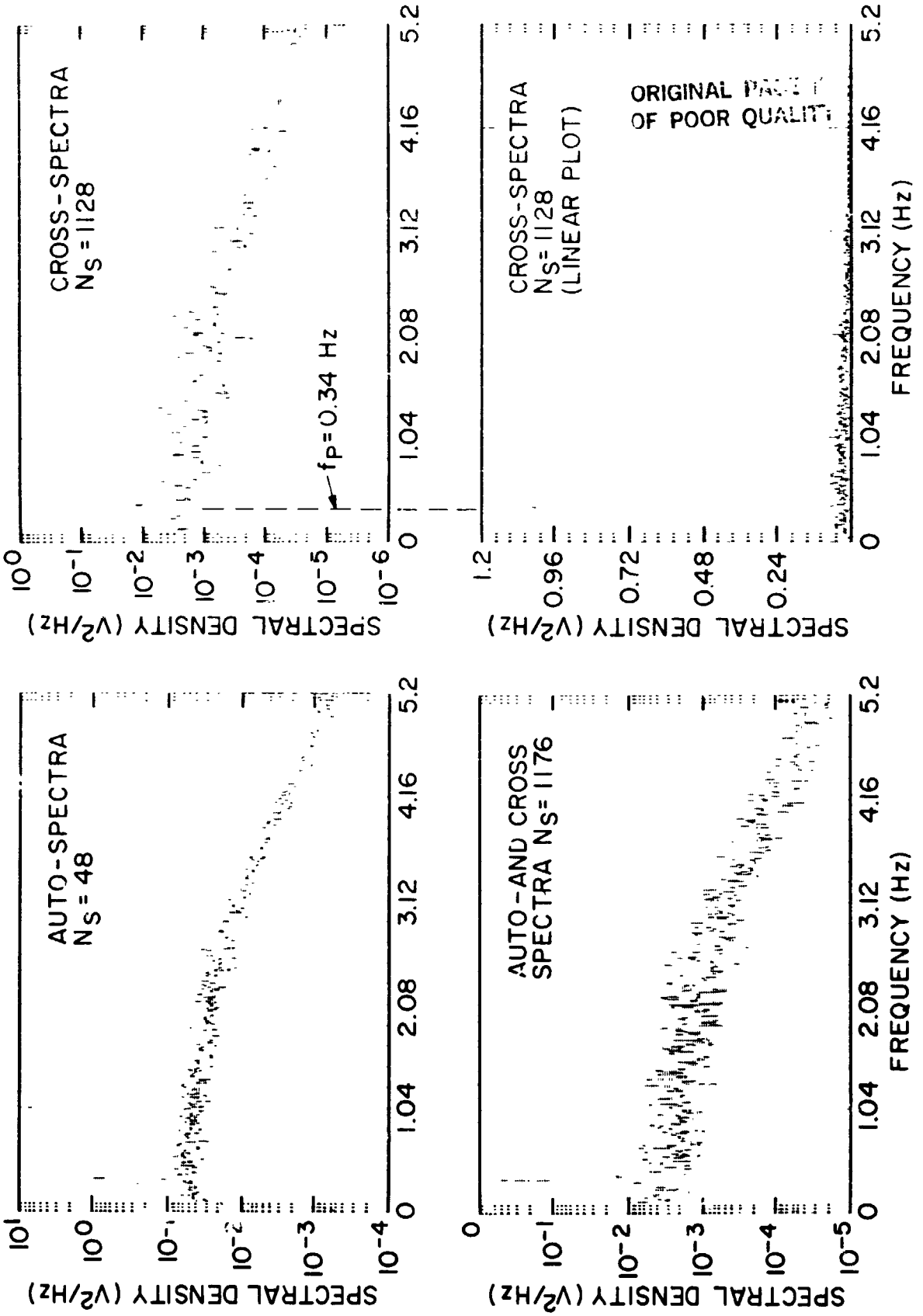


Figure 7 Computer processing of frequency-agile data. (a) Auto-spectra (standard mode), (b) spectrum resulting from summing auto- and cross-spectra for all possible carrier frequencies, (c) spectrum resulting from summing cross-spectra for all carrier frequencies greater than zero, and (d) spectrum of (c) on a linear scale.